Simulating thermal dynamics of the largest lake in the Caucasus region: The mountain Lake Sevan

Muhammed Shikhani,[1] Chenxi Mi,[1,2*] Artur Gevorgyan,[3,4] Gor Gevorgyan,[5] Amalya Misakyan,[3] Levon Azizyan,[3] Klemens Barfus,[6] Martin Schulze,[1] Tom Shatwell,[1] Karsten Rinke[1]

[1]Department of Lake Research, Helmholtz Centre for Environmental Research, Magdeburg, Germany; [2]College of Water Conservancy, Shenyang Agricultural University, Shenyang, China; [3]Hydrometeorology and Monitoring Center SNCO of the Ministry of Environment of the Republic of Armenia, Yerevan, Armenia; [4]School of Earth, Atmosphere and Environment, Monash University, Melbourne, Australia; [5]Scientific Center of Zoology and Hydroecology, National Academy of Sciences of Republic of Armenia, Yerevan, Armenia; [6]Institute of Hydrology and Meteorology, Technische Universität Dresden, Dresden, Germany

ABSTRACT

Lake Sevan is the largest freshwater body in the Caucasus region, situated at an altitude of 1,900 m asl. While it is a major water resource in the whole region, Lake Sevan has received little attention in international limnological literature. Although recent studies pointed to algal blooms and negative impacts of climate change and eutrophication, the physical controls on thermal dynamics have not been characterized and model-based assessments of climate change impacts are lacking. We compiled a decade of historical data for meteorological conditions and temperature dynamics in Lake Sevan and used a one-dimensional hydrodynamic model (GLM 3.1) in order to study thermal structure, the stratification phenology and their meteorological drivers in this large mountain lake. We then evaluated the representativeness of meteorological data products covering almost 4 decades (EWEMBI-dataset: 1979-2016) for driving the model and found that these data are well suited to restore long term thermal dynamics in Lake Sevan. This established model setting allowed us to identify major changes in Lake Sevan's stratification in response to changing meteorological conditions as expected from ongoing climate change. Our results point to a changing mixing type from dimictic to monomictic as Lake Sevan will experience prolonged summer stratification periods and more stable stratification. These projected changes in stratification must be included in long-term management perspectives as they will intensify water quality deteriorations like surface algal blooms or deep water anoxia.

Corresponding author: chenxi.mi@ufz.de

Key words: General Lake Model (GLM); Lake Sevan; temperature stratification; EWEMBI; climate warming.

Contributions: All the authors made a substantive intellectual contribution, read and approved the final version of the manuscript and agreed to be accountable for all aspects of the work.

Conflict of interest: The authors declare that they have no competing interests, and all authors confirm accuracy.

Citation: Shikhani M, Mi C, Gevorgyan A, *et al.* Simulating thermal dynamics of the largest lake in the Caucasus region: The mountain Lake Sevan. *J. Limnol. 2022;81(s1):2024.*

Edited by: Bardukh Gabrielyan, *Scientific Center of Zoology and Hydroecology, Division of Natural Sciences, Yerevan, Armenia.*

Received: 18 April 2021.
Accepted: 29 September 2021.

Publisher's note: All claims expressed in this article are solely those of the authors and do not necessarily represent those of their affiliated organizations, or those of the publisher, the editors and the reviewers. Any product that may be evaluated in this article or claim that may be made by its manufacturer is not guaranteed or endorsed by the publisher.

J. Limnol., 2022; 81(s1):2024
DOI: 10.4081/jlimnol.2021.2024

INTRODUCTION

Lake Sevan (Armenia) is the largest natural lake in the Caucasus and a unique water resource within a water-scarce region. Despite its importance for the region and its ecological significance as habitat for endemic and endangered species, the limnology of Lake Sevan has gained only little attention in the international scientific literature. This lake has tremendously suffered from unsustainable water abstractions for hydropower generation and irrigation, which lowered the lake level by almost 20 m, as well as from overfishing and eutrophication in the 1970s to 1990s (Gabrielyan *et al*., 2022; Hovhanissian and Gabrielyan, 2000). Recently, cyanobacterial blooms reoccurred in the summers of 2018 and 2019, pointing to another phase of eutrophication and environmental change (Gevorgyan *et al*., 2020). Besides intense nutrient loading of the lake, increasing summer water temperatures have been discussed as a potential driver of this new wave of cyanobacterial mass developments (Gevorgyan *et al*., 2020). This hypothesis was raised because the occurrence of cyanobacteria coincided with surface water temperatures reaching 25°C, which have rarely been recorded before. A broad body of evidence exists documenting the positive effects of warming on cyanobacterial

blooms (Hayes *et al*., 2020; Ho *et al*., 2019; Paerl and Huisman, 2008). This points to the increasing importance of climate warming for Lake Sevan and its ecosystem. Until 2100, a decrease of precipitation by 4.6% and river flow by 40.8% in parallel with an increase in evaporation by 17.8% had been estimated for Lake Sevan and its catchment (Yu *et al*., 2014). It has moreover been projected that Armenia will experience significant warming in the future, and air temperature at the end of the century can be 4-6 °C higher than current climate conditions (Gevorgyan *et al*., 2016). However, a quantitative assessment of climate warming effects on the water body of Lake Sevan is still missing. This study was designed to initiate such an assessment which focuses on the effects of warming on stratification, mixing, and thermal dynamics within this large mountain lake.

Thermal stratification, a key characteristic in determining lake structure, is sensitive to climate conditions (Woolway *et al*., 2021). The density gradient in a stratified lake controls the vertical transport of nutrients, dissolved gases, and other compounds and thus affects chemical and biological processes in lakes (*e.g.* Berger *et al*., 2014; Boehrer and Schultze, 2008; North *et al*., 2014). Generally, warming will increase stratification duration and stability (Kirillin, 2010; Mi *et al*., 2020) and can also induce changes in mixing type (Woolway and Merchant, 2019). Physical lake models, even in their simplest one-dimensional form have been shown to reproduce thermal dynamics with relatively high accuracy (Bruce *et al*., 2018; Mesman *et al*., 2020) and are hence well suited for studying future changes in lake stratification and mixing. Lake models are therefore an efficient tool to simulate the consequences of climate warming and have even been applied to develop adequate adaptation strategies (Mi *et al*., 2020).

The goal of this study was to develop, calibrate, and validate a 1D hydrodynamic model of Lake Sevan to describe the stratification characteristics and physical structure of the lake. We aimed to run long-term, *i.e.*, up to multi-decadal, simulations to characterize the effect of climate variability. Furthermore, we applied the model to quantify the sensitivity of the lake's physical structure against climate warming and changes in wind conditions. These tasks also included compiling all relevant meteorological, hydrological, and limnological data of this lake into one coherent simulation setting. An important aspect of our work was to elucidate to which extent a simple 1D lake model is sufficient to reproduce stratification dynamics given the fact that the meteorological conditions over the lake are considerably heterogeneous, and Lake Sevan is separated into two large sub-basins.

METHODS

Study site

Lake Sevan (central point 40.4° Latitude, 45.3° Longitude) consists of two sub-basins that are separated by a sill. The southern part, which is shallower (max. depth 32 m) and has a larger surface area (939 km^2), is commonly referred to as Big Sevan (Fig. 1). The second basin, Small

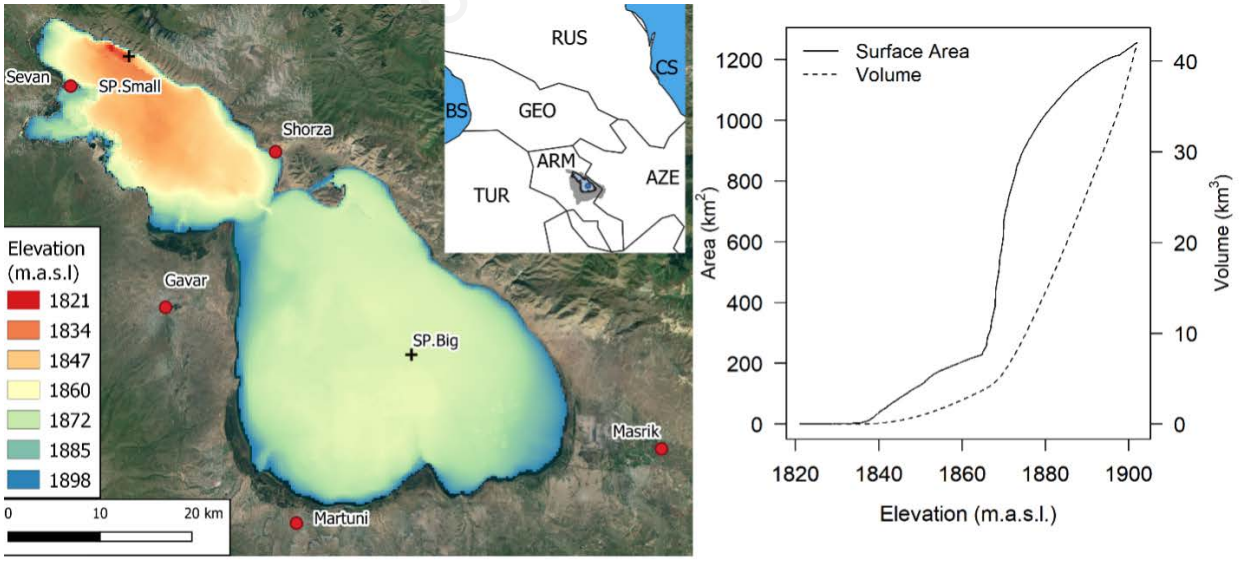

Fig. 1. Left: map of Lake Sevan (source for base map: aerial imagery by Google maps) including information on water depth as a color scale; the black crosses represent the sampling sites while the red points represent the location of the meteorological stations; the inset shows the location of Lake Sevan and its catchment within Armenia and the region where BS is the Black Sea and CS is the Caspian Sea. Right: a bathymetry function for surface area and volume (data source Hydrometeorology and Monitoring center HMC).

Sevan, is the deeper northern part that has a surface area of 338 km^2 and a maximum depth of 81 m located at the northeastern edge (Hovanesian and Bronozian, 1994). The relationship between surface area, accumulated volume and lake level is shown in Fig. 1. The total volume of the lake was assessed in 2019 to be 39 km^3 according to Andréassian *et al*. (in press). Lake Sevan is dimictic, however, complete ice cover occurs only exceptionally (Andréassian *et al*., in press; Poddubny, 2010). In the second half of the twentieth century, Lake Sevan experienced a drawdown of its water level by up to almost 20 m and eutrophication in parallel (Gabrielyan *et al*., 2022). In recent years, cyanobacterial mass developments occurred again (Gevorgyan *et al*. 2020), causing a decline in water quality, including considerable variation of Secchi depth within the course of the year (see section "Model setup and forcing data" below).

Lake Sevan water balance and hydrology

The lake has 28 inflowing rivers and one water diversion tunnel (Arpa-Sevan water canal), which delivers water from a neighboring catchment. Twelve of the inflows are gauged and constitute nearly 80% of the total inflow into the lake. The inflow discharge from the ungauged streams and the direct catchment inflow are estimated based on the discharge conditions in the gauged catchment (Q_{gauged}) according to the Hydrometeorology and Monitoring Center state non-commercial organization of the Ministry of Environment of the Republic of Armenia (HMC):

$$Q_{ungauged} = 0.1581 Q_{gauged} + 1.41\ m^3\ day^{-1} \quad \text{eq. 1}$$

Based on the data provided by HMC for the period 2008-2017, the total annual average inflow into Lake Sevan from both gauged and ungauged sources is estimated as 919.6 10^6 m^3 yr^{-1}. Furthermore, Lake Sevan has one outflow (River Hrazdan) with an annual average flow of 215.6 10^6 m^3 yr^{-1}. Based on the total annual inflow volume, the water body of Lake Sevan would have an average residence time of 42.4 years, while based on the annual average outflow, the residence time computes to 180 years, *i.e.*, more than four times longer. This large difference between inflow *vs.* outflow-based residence time estimates is typical for lakes in arid climates that have relatively high evaporation rates. Note that the definition of residence time is based on using the real flow-through of the system, which must be based on the outflow discharge. Therefore, the water residence time of Lake Sevan is correctly stated as approximately 180 years.

According to HMC, direct precipitation on the lake surface is estimated to be 80% of the average precipitation measured at the meteorological stations surrounding the lake. Altogether, Lake Sevan's annual average water budget between 2008 until 2017, in addition to the inflows and the outflow mentioned above, an annual average precipitation of 500 10^6 m^3 year^{-1}, and a calculated evaporation of 976.4 10^6 m^3 year^{-1}. However, the effective evaporation in the simulations is calculated according to the simulated water temperatures and meteorological conditions (Hipsey *et al*., 2019) and can deviate from the theoretical value that is closing the hydrological budget. As a result, modelled and observed water level dynamics might not show a perfect fit.

The hydrodynamic model

To simulate the hydrodynamics and thermodynamics in Lake Sevan, we selected an open-source, well-established lake model, the General Lake Model (GLM) version 3.1. GLM is a one-dimensional lake model developed by the Aquatic Eco Dynamics Research group at the University of Western Australia (Hipsey *et al*., 2019). The model, with its documentation and source code, is freely available at http://aed.see.uwa.edu.au/research/models/GLM. GLM has been widely applied to study both hydro-thermal dynamics and water quality in lakes and reservoirs worldwide (Bueche *et al*., 2017; Fenocchi *et al*., 2018; Mi *et al*., 2018; Weber *et al*., 2019). A community-effort to confront GLM with a data set of 32 very different lakes documented that GLM has a high transferability because it was able to simulate hydrodynamics in most of the systems with very high accuracy (Bruce *et al*., 2018). This proven transferability was a major argument for choosing GLM for this modelling study.

GLM simulates the dynamics of the water balance, mixing, and thermal structure of the lake. The model accounts for surface mass and energy fluxes as well as inflows/outflows, and considers the effect of ice cover. The surface heat fluxes are composed of shortwave radiation, longwave radiation, latent heat, and sensible heat. The model applies a Lagrangian layer structure, in which the layer thickness can change during the runtime of the model by shrinking and expanding certain layers due to water volume changes. At a specific, user-defined, critical layer thickness, a layer can be split into two new layers if it surpasses the defined maximum layer thickness, or two neighboring layers can be merged if they get smaller than the defined minimum layer thickness. Accordingly, the number of layers and their vertical structure change dynamically during the simulation. We specified meteorological inputs and model outputs at hourly resolution, which facilitates accounting for sub-daily dynamics. Further information about the model equations, algorithms, and sub-modules is presented in Hipsey *et al*. (2019).

Model setup and forcing data

Our initial model setup included a simulation period of ten years from 2008 until the end of 2017. The model was driven by input data for the morphometric, hydro-

logic, and meteorological conditions. The morphometry of the lake was introduced to the model *via* the bathymetric curve shown in Fig. 1 using data provided by HMC.

The inflows, the outflow, and the inflow temperatures were provided as well by HMC as a time-series at a daily resolution. The inflow files of the 12 gauged rivers were provided to the model, as well as a 13th inflow file that was derived to represent the ungauged inflows and the direct catchment according to eq. 1.

The meteorological data driving the model were retrieved from 5 stations distributed around Lake Sevan at varying altitudes (Fig. 1). These stations are characterized by systematic differences in meteorological variables arising from local meteorological features. Inspection of the individual data for each of the meteorological stations revealed that Masrik station, located in the southeast, showed significantly higher wind speed. These wind conditions in Masrik station are associated with topographically induced funneling effects arising from regional-scale heat-driven circulation between the Armenian Highland and Kura-Araks plain and the Caspian Sea (Gevorgyan and Melkonyan, 2015). In general, wind speed appeared to be the meteorological variable with the highest interstation variability as indicated by the highest coefficient of variation of approximately 30% (Tab. 1).

Lake Sevan was initially simulated using each meteorological station separately in order to characterize the effects on thermal and water level dynamics. The model parameters were assigned to default values as mentioned by Hipsey *et al*. (2019). The results of these simulations demonstrated, as expected, substantial variations in lake water temperatures and water levels arising from the contrasting meteorological conditions at the different meteorological stations. In order to achieve a meteorological data set that can be considered representative for the whole lake, we calculated the arithmetic mean from all stations to force the model. The averaging approach aimed to attain a more accurate representation of the meteorological conditions but, of course, represents a compromise that cannot fully take into consideration the spatial heterogeneity of meteorological conditions over the large surface area of the lake. However, we consider the arithmetic mean to be an acceptable assumption since a more complex method will not significantly improve the simulation results from a 1D model, but this might not be true for a 3D model setup with heterogeneous wind fields. This synthetic station is referred to as "Average". Test simulations by the model were used to evaluate the representativeness of the "Average" meteorological input data set. As alternative meteorological input, the global dataset of EartH2Observe, WFDEI and ERA-Interim data Merged and Bias-corrected for ISIMIP (hereafter EWEMBI) was used as well to drive the simulation of Lake Sevan, EWEMBI data had a reasonable correlation with the Average local meteorological input between 2008 and 2016 (Tab. 1). The systematic over/underestimations are expressed with the overall bias between EWEMBI and the average meteorology ($\overline{EWEMBI} - \overline{Average}$) (Tab. 2).

The meteorological variables of air temperature, relative humidity, wind speed, precipitation, and cloud cover were obtained from the stations at a three-hour resolution. To improve the performance of the model and capture the diurnal conditions in the lake, the data were disaggregated into hourly resolution by linear interpolation.

The longwave radiation was chosen to be internally calculated within the model via cloud cover by following the approach of Swinbank (1963). Since shortwave radiation (R) was not measured at any of the meteorological stations, we estimated R based on a three-step approach. First, the solar angle ϕ (in degree) was calculated based on time and location using the approach by Michalsky (1988). Second, the resulting clear sky radiation R_0 (in W m^{-2}) from the given solar angle was calculated by the following equation (modified from Kasten and Czeplak, 1980):

Tab. 1. Average values of meteorological variables retrieved from the five stations around Lake Sevan for the period 2008-2017 (for EWEMBI 2008-2016). Standard deviation was calculated using the station-specific averages.

Station		Altitude (m asl)	Shortwave radiation (W m^{-2})	Cloud cover (fraction)	Air temperature (°C)	Relative humidity (%)	Wind speed (m s^{-1})	Precipitation (mm)
Gavar		1961	184.4	0.48	5.5	71.5	1.4	513.2
Sevan		1917	171.7	0.53	6.6	73.1	1.8	589.4
Shorza		1917	180.5	0.478	7.2	73.9	2.3	362.6
Martuni		1943	164.7	0.55	6.8	66.7	2.5	566.9
Masrik		1940	190.4	0.44	5.5	65.1	3.4	460.4
Average	Mean		178.3	0.49	6.3	70.0	2.3	498.5
	Standard deviation		10.16	0.04	0.77	3.97	0.77	90.91
	Coefficient of variation (%)		5.7	9.5	12.3	5.6	33.3	18.2
EWEMBI			167.0	0.77	6.0	71.0	1.8	557.4

$$R_0 = 990\phi - 30 \quad \text{eq. 2}$$

Third, the shortwave radiation R (in W m^{-2}) was calculated from clear sky radiation and cloud cover (n, given as fraction, *i.e.* 0…1) according to Kasten & Czeplak (1980):

$$R = R_0\,(1 - 0.75n^{3.4}). \quad \text{eq. 3}$$

The daily averaged values of the final meteorological input data are shown in Fig. 2. Wind speed showed a daily mean of 2.25±1 m s^{-1}, and only 0.1% of the total measurements showed values less than 0.5 m s^{-1}. Therefore still-air limit was neglected. The large surface area of Lake Sevan is another reason for not considering both still-air limit and wind sheltering. Moreover, the non-neutral atmospheric stability was not considered, owing to the long simulation period.

The light extinction coefficient (k_W) value was set to 0.35 m^{-1} throughout the simulation. This value was based on available monthly Secchi depth measurements in both Big Sevan and Small Sevan between December 2017 and December 2018 and between April and September 2019 with some gaps in Big Sevan for this period. The annual mean of Secchi depth observations in Big Sevan is 4.7±1.5 m and in Small Sevan, 5±2.2 m. According to Poole and Atkins (1929), the light extinction coefficient (k_W) can be calculated from Secchi depth (S_d) by:

$$k_w = 1.7/S_d \quad \text{eq. 4}$$

Model calibration and evaluation

For calibration we used the vertical temperature profiles which were provided by HMC at a monthly resolution at the deepest point in Small Sevan (referred to as SP.Small as shown in Fig. 1) at different depths (0.1 m, 5 m, 10 m, 20 m, 30 m, 40 m, 50 m, 77 m). For evaluating

Tab. 2. Correlation and bias between the meteorological variables from the EWEMBI data and the averaged measured meteorology for Lake Sevan.

Variable	Unit	Coefficient of determination R^2	Bias
Air temperature	°C	0.97	-0.296
Shortwave radiation	W m^{-2}	0.82	-10.1
Cloud cover	fraction	0.15	0.27
Wind speed	m s^{-1}	0.27	-0.5
Relative humidity	%	0.48	1.07
Precipitation	mm	0.36	31.8

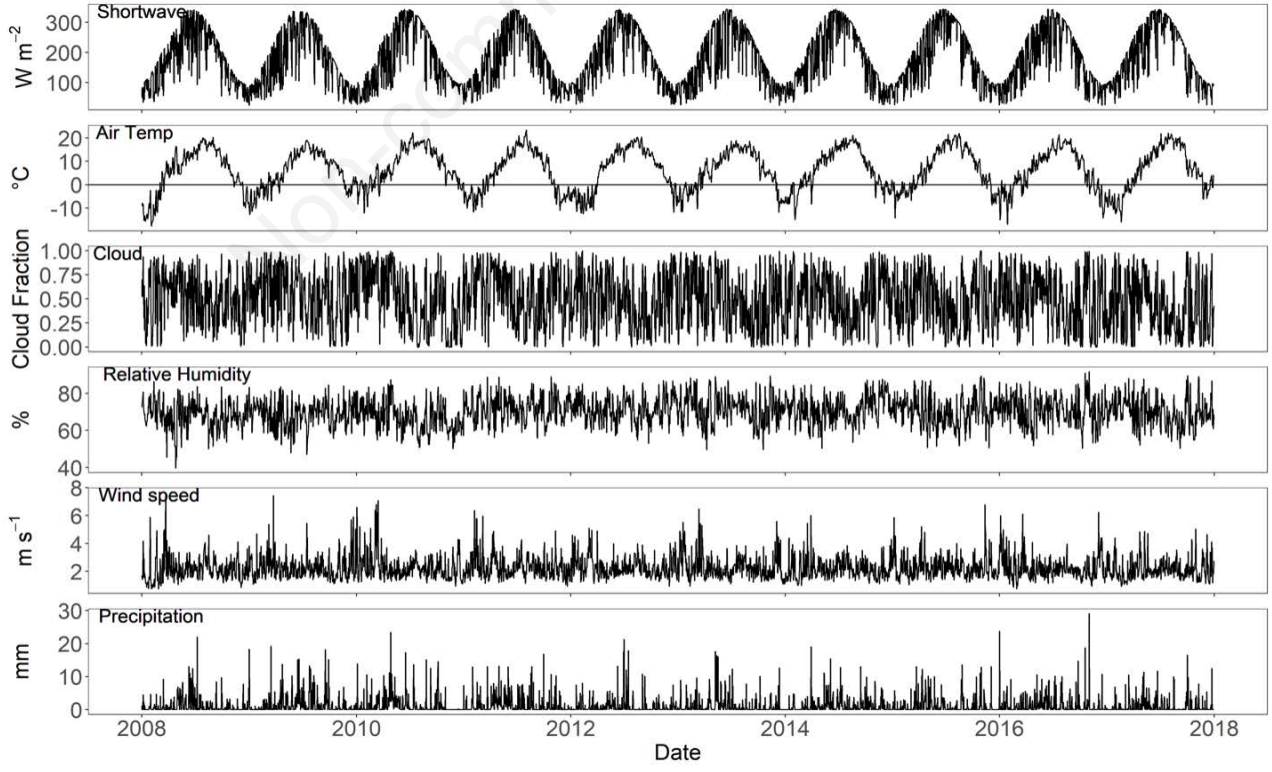

Fig. 2. Daily averaged meteorological input variables.

the model performance we also compared the output with the vertical profiles taken at the central area of Big Sevan (referred to as SP.Big), with the same temporal resolution at different depths (0.1 m, 5 m, 10 m, 20 m, 32 m) as well as the data from SP.Small.

The simulation based on measured local meteorology period started in January 2008 and terminated in December 2017. The simulation was initiated on January 1st 2008 with a homothermal condition of 4°C over the entire profile as these are typical temperature conditions in Lake Sevan at this time of the year.

The initial simulations showed systematically higher surface temperatures as well as notably higher water levels compared to observations. This points to a systematic error in the heat and water balance which likely results from an underestimation of the evaporative flux. We therefore calibrated the following three parameters that, among other processes, also affect evaporative fluxes: the wind factor *WF*, the hypolimnetic vertical diffusion coefficient C_{hyp}, and the latent heat drag coefficient c_e. The latent heat drag coefficient has a significant effect on the evaporative flux, and thus it allowed us to gain a better reproduction of the observed water level, as well as its cooling effect which also helped against the systematic overestimation of surface temperatures. The wind factor was calibrated to account for the high variability among the meteorological stations in terms of wind speed (Tab. 2), and to compensate the over cooling/warming induced by the c_e. The initial simulations showed strong local temperature gradients, which prompted the calibration of the vertical diffusion coefficient. We used the calibration function from the R package "glmtools" following the method by Ladwig *et al*., (2021, 2018) and employed the Covariance Matrix Adaption Evolution Strategy (CMA-ES) algorithm (Hansen, 2016). The process was carried out by dividing the simulation period into a calibration period from 2008-2014 and a validation period between 2015-2017 (using 200 iterations). The value of c_e after calibration reached about 0.0026 instead of 0.0013 in the default, which is in the range of other studies using GLM (Ladwig *et al*., 2018; Rinke *et al*., 2010). Similarly, the hypolimnetic vertical diffusion coefficient post-calibration was at 6.79 10^{-5} m^2 s^{-1}, consistent with the range in the literature (Dong *et al*., 2020). The wind factor WF slightly changed post-calibration to 0.97.

The model performance was evaluated using model bias and the root mean squared error RMSE.

$$bias = \overline{S} - \overline{O} \qquad \text{eq. 5}$$

$$RMSE = \left(\frac{\sum(S_i - O_i)^2}{n}\right)^{\frac{1}{2}} \qquad \text{eq. 6}$$

where (S_i) and (O_i) are the simulated and the observed values, ($\overline{S}$) and ($\overline{O}$) are their arithmetic means, respectively, and n is the sample size.

The stratification of Lake Sevan was evaluated based on the output of the simulations. The lake was defined in a stratified state when the density difference, calculated from water temperatures, between 0 m and 30 m was higher than >0.02 kg m^{-3}. This density difference threshold corresponds to the temperature difference of 1K around the end of April when surface temperature is about 6°C. Note, that prominent lake modelling studies used such a 1K-rule for determining stratification (Fang and Stefan, 2009). Moreover, a density-based threshold ensures a more robust criterion to determine both summer and winter stratification and the chosen value of >0.02 kg m^{-3} fits well to the climatic and morphometric conditions of Lake Sevan. We assumed that the stratified state occurs only when both basins are stratified, therefore the calculations were based upon the temperature retrieved from 30 m depth as an acceptable value that represents bottom temperature conditions in Big Sevan and clearly hypolimnetic conditions in Small Sevan. The stratification duration is taken as the longest uninterrupted stratification period and the onset (offset) of stratification is specified as the first (last) day of this period. Stratification key events and indices were defined and analyzed using stratification analysis tools from the R-package "LakeEnsemblR (Moore *et al*., 2021) following related studies (Shatwell *et al*., 2019; Wilson *et al*., 2020).

Moreover, the strength of stratification was characterized by Schmidt stability (Idso, 1973; Schmidt, 1928) that was calculated by:

$$s = \frac{g}{A_0}\int_0^{z_{max}} (z - z_c)(\rho_z - \rho_c)A_z dz \qquad \text{eq. 7}$$

where g (m s^{-2}) is the gravitational acceleration, A_0 (m^2) the surface area, A_z and ρ_z (kg m^{-3}) are the area and the density of the water at the depth z, respectively. z_c (m) is the depth of the center of gravity of the entire lake volume and ρ_c is the density at depth z_c with the latter given by:

$$z_c = \frac{\int_0^{z_{max}} zA_z dz}{\int_0^{z_{max}} A_z dz} \qquad \text{eq. 8}$$

Multi-decadal simulation setup

In a second model application, based on the calibrated model parameters, we established a multi-decadal simulation by using EWEMBI data (Lange, 2019) as meteorological input. The EWEMBI data is a global dataset that has a spatial resolution of 0.5° degrees and a daily tem-

poral resolution spanning from 1979 until 2016. EWEMBI was produced by merging meteorological forcing data and ERA-Interim reanalysis data as part of the ISIMIP project. We downscaled the gridded data of 0.5° resolution to the lake's center via bilinear interpolation using climate4R bundle of packages (Iturbide *et al*., 2019) (https://github.com/SantanderMetGroup/climate4R). EWEMBI showed a very good agreement with the "Average" station data, except for cloud cover, wind speed and precipitation, which were overestimated (Tab. 2). This agreement allowed us also to run the model for the whole period covered by EWEMBI (1979-2016), *i.e.*, over almost four decades. Our intention behind this multi-decadal simulation was twofold; we aimed to i) test to which extent gridded meteorological data products can substitute meteorological observations, and ii) achieve more robust statistical analysis of the stratification phenology in Lake Sevan by increasing the length of the time series. Note, however, that EWEMBI data product is only available at daily resolution. GLM allows using daily resolved meteorological input data as it contains an internal mechanism for disaggregation into sub-daily time-steps (Hipsey *et al*., 2019). For this purpose, we ran GLM in the mode of daily-resolved meteorological inputs when simulating with the EWEMBI dataset.

We lacked hydrological data for Lake Sevan over the four decades of the EWEMBI simulation. Given the long residence time of water in Lake Sevan and the relatively small inflow/outflow volumes compared to the lake volume we simplified the setting in such a respect that we set inflows and outflow to zero and turned off the precipitation and evaporative mass loss resulting in a constant water level throughout the simulation period (taking the initial water level in 2008 as starting value). The latter is a new feature in GLM 3.0 that allows evaporative mass losses from the surface layer to be excluded from the water budget, but the evaporative heat loss is always included in the heat budget. Note, that in this simplified setting, water level fluctuations are not occurring and levels remain constant over the whole simulation period. The effects on thermal dynamics can, nevertheless, be considered to be negligible as heat import/export by inflows and outflows is several orders of magnitude lower than heat exchange with the atmosphere.

Scenario description

In order to examine the response of Lake Sevan to a warming climate, the sensitivity of the lake's thermal structure against increasing air temperatures was analyzed. Therefore, using the calibrated model with averaged meteorological forcing, the air temperature was increased over a range of 1 to 5 K with an interval of 1 K. The remainder of the meteorological variables were left unchanged. Note that humidity is given as relative humidity and a temperature increase implies that vapor pressure is rising, as well, if the relative humidity is kept the same. This is meaningful because otherwise (*i.e.,* keeping vapor pressure constant during temperature increase), evaporative fluxes increase disproportionally and potentially distort the direct effects from the temperature change.

Despite the simplicity of this assumption it has been frequently used in previous studies (*e.g.*, Farrell *et al*., 2020; Kerimoglu and Rinke, 2013). Although there is no consideration of seasonal differences in warming rates or changes in other variables than air temperature, it represents a useful way to examine the sensitivity of stratification phenology to warming without potential distorting effects from other variables or more complex meteorological dynamics. Moreover, its simplicity is helpful to keep the results easily interpretable by lake managers and to have a straightforward scenario design where only one variable is changed at a given time. Additionally, the suggested warming scenarios up to +5 K are in accordance to the assessment of projected temperature changes in Armenia where warming is expected in the summertime to reach values greater than 4 K for the worst case scenario (Gevorgyan *et al*., 2016; Vardanyan *et al*., 2014; Vermishev *et al*., 2015).

Given the large spatial variability of wind in the Sevan region (Tab. 1), we also included a sensitivity study on wind speed and changed the wind speed by ± 10% and 20% because any climatic change can also have strong effects on the local wind field potentially leading to distinct changes of average wind conditions on the lake. Both warming and wind scenario results were analyzed with respect to water surface temperature responses, as well as stratification duration, date of stratification onset and end, the stability of the stratification, and the mixing layer depth.

All analyses were performed with R version 4.1.0 (R Core Team, 2021; RStudio Team, 2021). The R packages "GLM3r", "glmtools", "Climate4R" bundle of packages (Iturbide *et al*., 2019), "LakeEnsemblR"(Moore *et al*., 2021), and "rLakeAnalyzer" (Winslow *et al*., 2014) were used for running the simulation, pre and post-processing and for computing the above-mentioned indices. For testing monotonic trends in the long-term simulations we used Mann-Kendall test (Sen, 1968) from R package "trend" and the magnitude of it was calculated using Sen's slope method from R package "zyp".

RESULTS

Identification of a representative meteorological input

The simulations using the calibrated parameters and the meteorological inputs from the five meteorological stations produced considerable variation in simulated water temperatures. We transformed modeled surface

water temperatures over the simulated 10 years into an average annual cycle by using a circular general additive model (GAM) in order to illustrate the differences. While simulated surface water temperatures using data from Masrik station were far colder than the others, due to very high wind speed and resulting higher evaporation, Gavar station produced very high surface water temperatures owing to low wind speed (Fig. 3, Tab. 1). Simulated water levels using the 5 different meteorological stations were also very different, and Masrik station, with its higher wind speed and corresponding higher evaporation, even showed a negative water balance. While water levels in the Shorza- and Masrik-simulation dropped by approximately 1 m and 2 m, respectively, over the ten years of simulation, all other stations, including the averaged setting, resulted in relatively well-fitting water levels.

When driven by the averaged meteorological setting, GLM reproduced the water level dynamics with reasonable accuracy and much better than any simulation driven by an individual station. The difference between

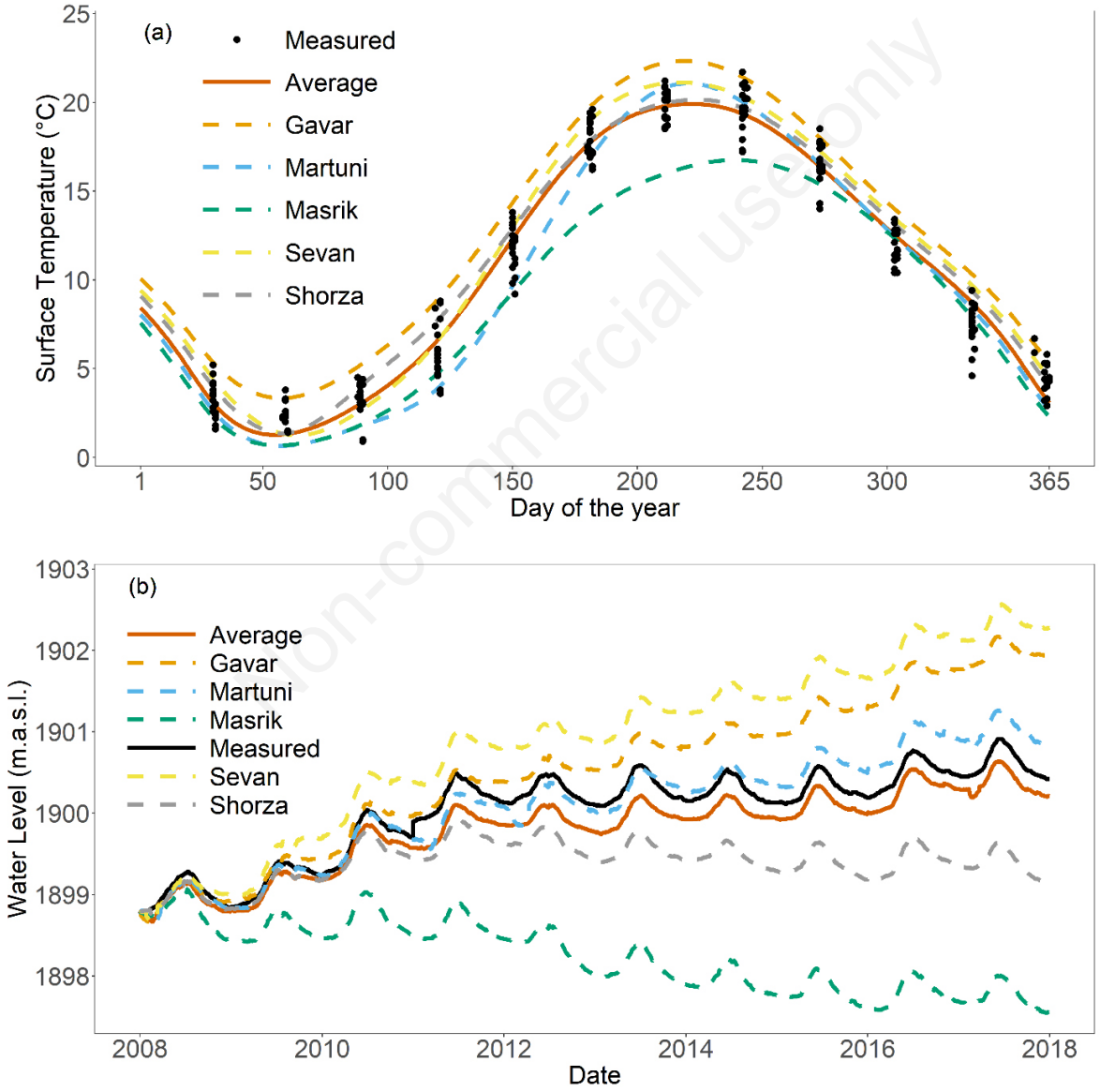

Fig. 3. a) Comparison of seasonally averaged surface water temperatures based on a cyclic GAM of simulations using the different meteorological stations against surface water temperature observations from SP.Small and SP.Big. b) The corresponding water levels of the simulations using the different meteorological stations against observations.

the simulated and the observed water level at the end of the simulation was only 0.2 m corresponding to an average bias of 2 cm per year (Fig. 3b). Between the years 2011 and 2015, the model showed a slight underestimation of the water level, but identical trends, seasonality, and peaks. The simulated surface water temperatures using the averaged meteorological data showed a seasonal pattern that was in good agreement with observations (points in Fig. 3a). However, the model slightly underestimated the surface water temperature during the second half of winter and overestimated it during the autumn. But still, compared to the simulations driven by individual meteorological stations, the averaged setting performed far better. We concluded that the averaged meteorological conditions provide the best descriptor of the meteorological conditions at Lake Sevan and, therefore, we further used averaged meteorological conditions in the simulations.

Model performance of the reference simulation from 2008 until 2017

The modeled water temperatures were in good agreement with the measured temperatures in all depths as indicated by R^2 values of 0.89 in Big Sevan and 0.91 in Small Sevan (Fig. 4). The corresponding RMSEs amounted to 1.56°C for Small Sevan and 1.85°C for Big Sevan for the total duration of the simulation (RMSE for the calibration period was 1.48°C and for the validation period 1.73°C for Small Sevan). Nevertheless, the same pattern of underestimation of temperatures during winter is noticed in (Fig. 4), as well as the overestimation in autumn, especially in the deeper part of the lake. When averaged over time and depth, the model showed only a minor positive bias, which accounted to only 0.05°C for Small Sevan (mean simulated temperature: 8.53°C, observed mean temperature: 8.48°C) and 0.46°C for Big Sevan (mean simulated temperature: 9.68°C, observed mean temperature: 9.23°C). Note, that observed temperatures in Big Sevan are on average 0.8 K warmer than in Small Sevan due to the difference in depth and the fact that deeper layers (*i.e.*, profiles at Small Sevan) do not experience high rates of warming.

Comparing simulated and observed vertical temperature profiles on different dates showed that the dynamics in stratification were also well reproduced by the model (Fig. 5). Although deviations between modelled and observed temperatures were a bit higher in the metalimnion compared to surface and bottom layers (Fig. 5), the thermocline, the temperature gradients, and the seasonal development were in good agreement with the observations.

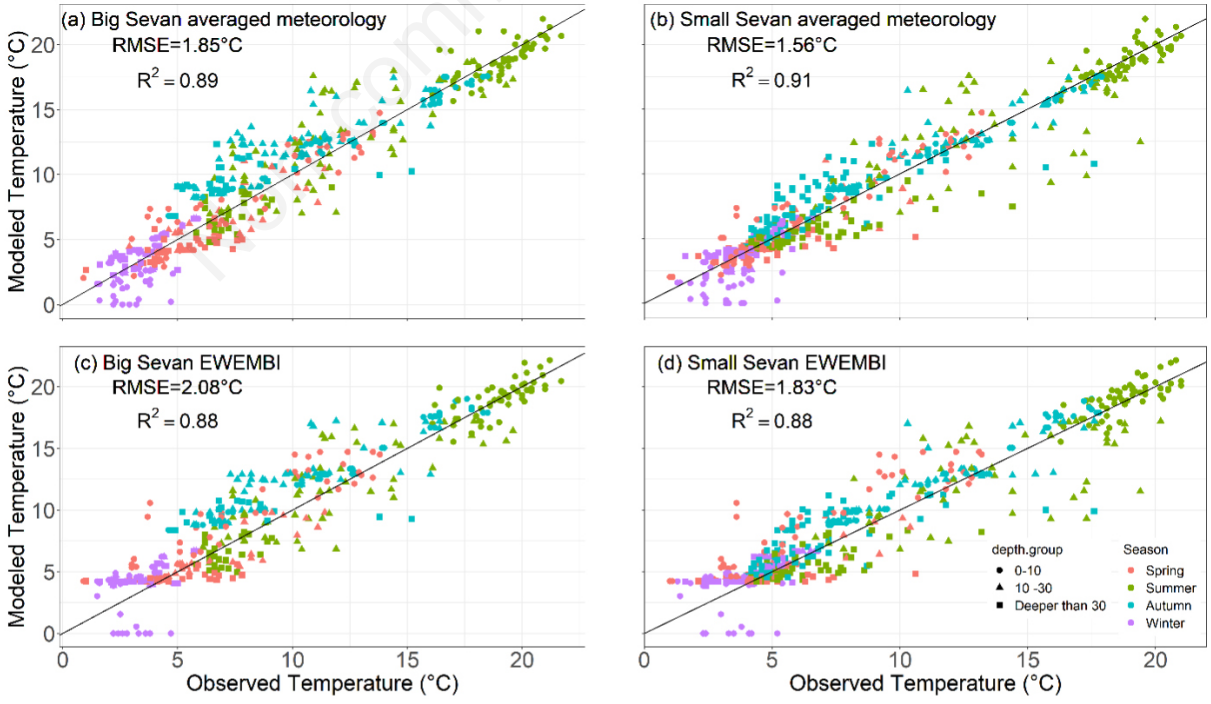

Fig. 4. Comparison between simulated and measured water temperatures for all depths. Left in Big Sevan and right for Small Sevan. a,b) Simulations driven by averaged meteorology. c,d) Simulations driven by EWEMBI meteorological data and excluding the water mass fluxes and flows.

Multi-decadal simulations using the EWEMBI-data as meteorological input

When using the EWEMBI data as meteorological inputs for the period from 2008 until 2016 (EWEMBI data end by 2016 and are therefore not available for 2017 and the temporal overlap in water temperature data between simulation and observation is in this case only 9 years), the model still satisfactorily captured water temperatures in the lake (Fig. 4). The model outputs for the EWEMBI-driven simulation were comparable to the simulations using the averaged measured meteorological data (2008-2017). Also the bias in water temperatures between simulation and observation remained in the same range as in the simulation using averaged measured meteorology which accounted to 0.27°C for Small Sevan (mean simulated temperature: 8.75°C, observed mean temperature: 8.48°C) and 0.77°C for Big Sevan (mean simulated temperature: 10°C, observed mean temperature: 9.23°C). For Big Sevan, the RMSE between observed and simulated temperature was 2.08°C and R^2 was 0.88, while for Small Sevan the agreement was better with a R^2 of 0.89 and RMSE of 1.83°C. The time series of the water temperature of the EWEMBI-driven simulation showed a very good agreement between the dynamics and

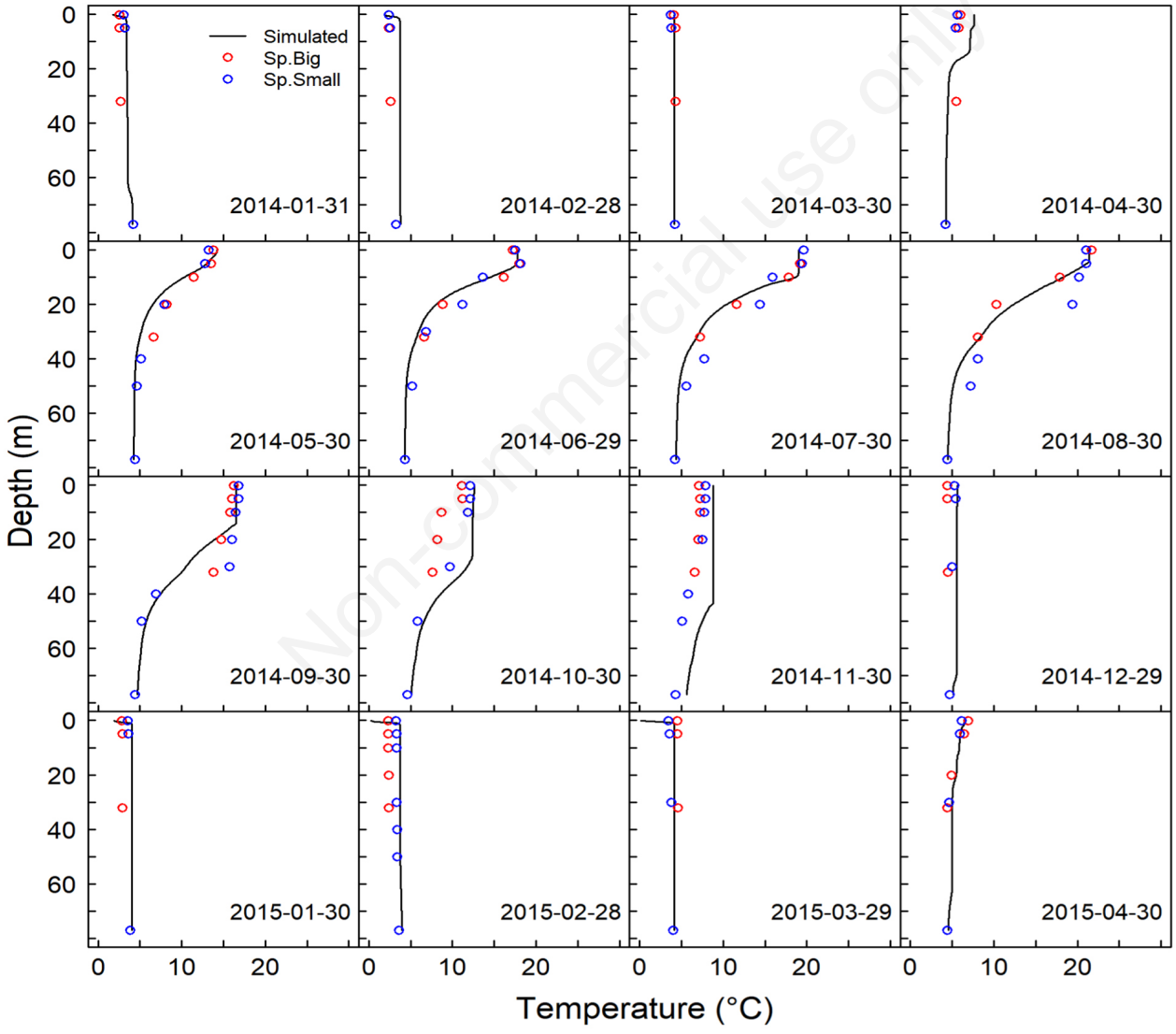

Fig. 5. Exemplary selection of simulated and observed temperature profile in Big and Small Sevan for the period from January 2014 until April 2015. Note that observations from both, Small and Big Sevan, are included in the graph. The respective observation date is given within each subplot.

seasonality of the simulated and observed surface and bottom water temperatures (Fig. 6). We therefore conclude that the EWEMBI data are representative for the local meteorological conditions at the lake and provide a reliable data basis for characterizing stratification phenology in Lake Sevan. Most notably, such gridded data products like EWEMBI can be almost as good as locally measured meteorological data when it comes to driving lake models. Long-term simulations from 1979 to 2016, *i.e.*, when using the full time period covered by EWEMBI, reflect the interannual variability of seasonal water temperature dynamics in Lake Sevan. Maximum surface water temperatures in this period were between 20°C and 23°C and the lake displayed winter inversed stratification in every year (Fig. 6).

We detected a statistically significant positive trend for surface temperature across the 38 years of simulation using the EWEMBI-data ($p<0.001$, Mann-Kendall, Sen's slope = 0.12 K decade^{-1}), which corresponds to a gross increase in surface temperature by 0.47 K between the beginning and the end of the simulation. Although the Mann-Kendall test also showed a significant increase in bottom temperature ($p<0.001$), Sen's slope value was in turn very low (0.003 K decade^{-1}) which indicates a very minor increase in bottom temperature of only 0.01 K from 1979 to 2016. The air temperature in EWEMBI exhibited an increasing trend, as well, where Sen's slope= 0.33 K decade^{-1} which resulted in an overall increase of 1.28 K from 1979 to 2016 indicating that warming is more pronounced in air temperature than in water temperature.

Stratification phenology

The simulated annual cycle of water temperatures characterized Lake Sevan as a classical dimictic lake with strong stratification during summer and a pronounced inverse stratification in winter (Fig. 7). Field observations

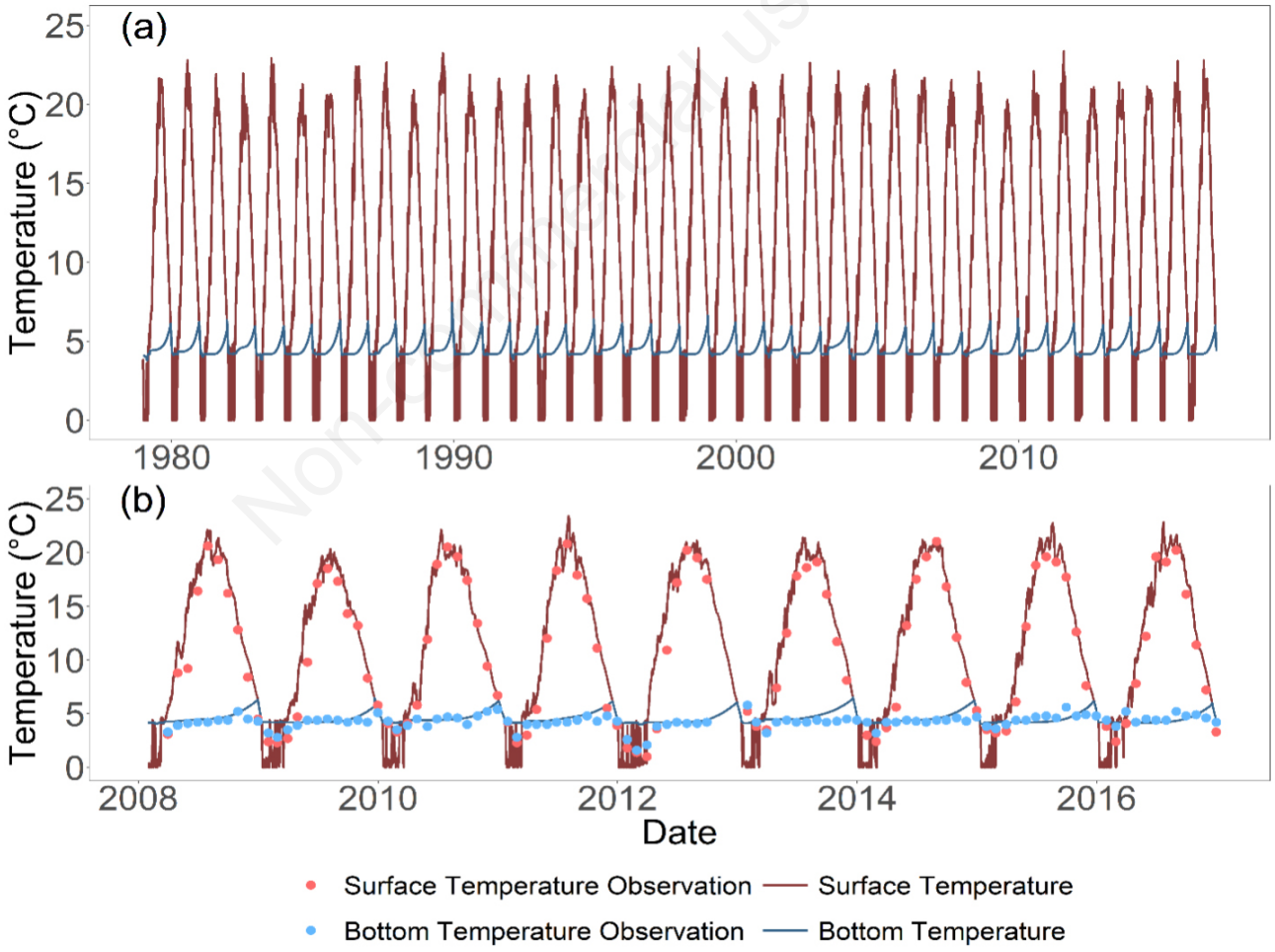

Fig. 6. a) Simulated surface and bottom (77 m) water temperatures (red and blue lines) for the period 1979 to 2016 with meteorological input data provided by EWEMBI. b) The simulated surface and bottom temperature between 2008 to 2016 including observed water temperatures added as red (surface) and blue (bottom; 77 m) circles.

indicate that Lake Sevan is not completely ice-covered in every winter but at least some parts of the lake freeze in every winter given the cold winter temperatures in 1900 m asl altitude in the Caucasus. We are lacking, however, a detailed record of ice dynamics and therefore cannot evaluate the outputs of the ice model.

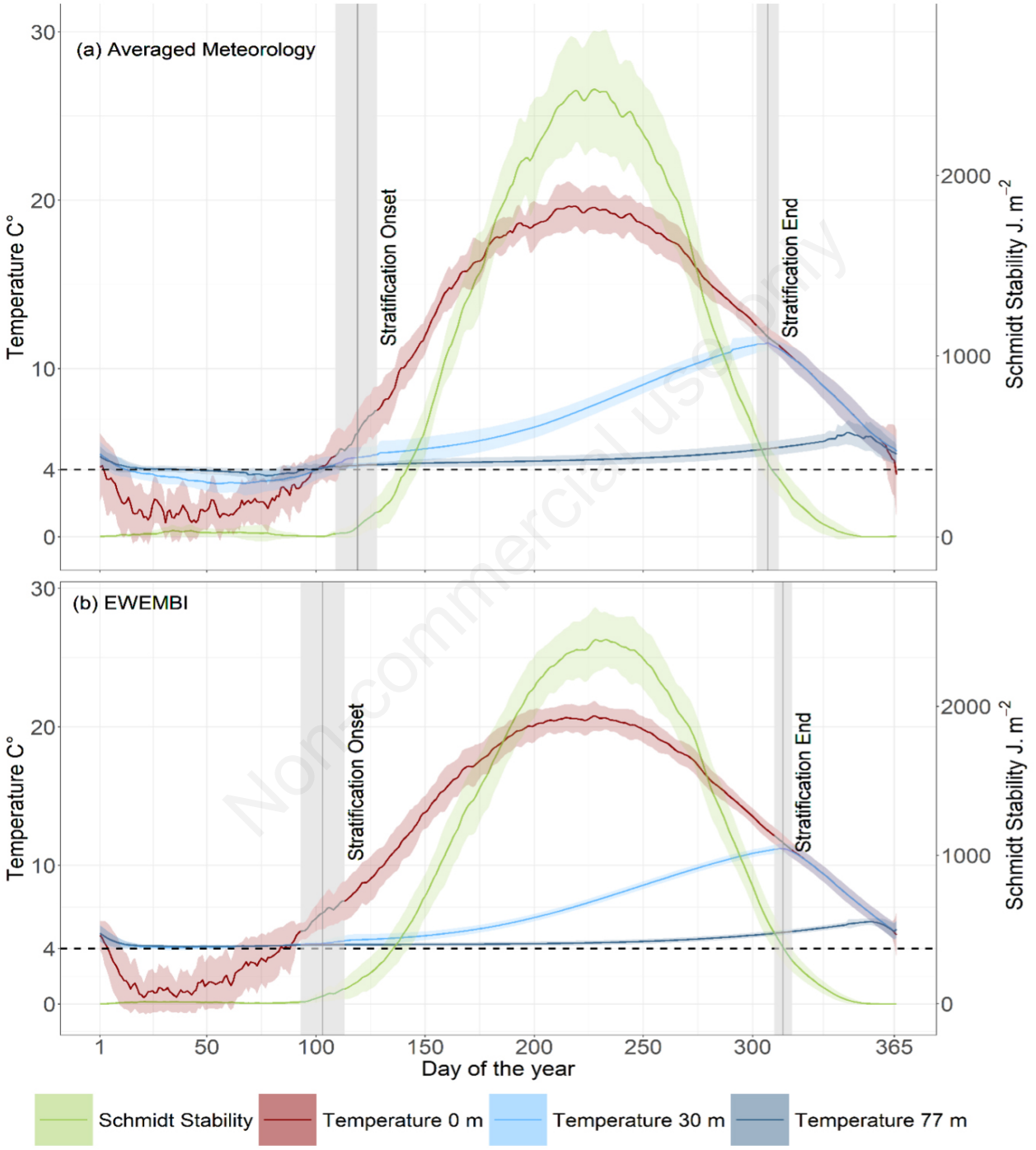

Fig. 7. The simulated annual cycle of stratification phenology of Lake Sevan as characterized by water temperatures at 0, 30, and 77 m depth and Schmidt stability. a) Simulation results using the averaged observed meteorology (2008-2017). b) Simulation results for using the multi-decadal EWEMBI data (1979-2016) as meteorological input. The lines represent the means and the shaded areas represents the standard deviation of the variables.

Summer thermal stratification started around the end of April or beginning of May (*i.e.*, approximately at the day of the year 119±10 days), and terminated around the end of October or beginning of November (*i.e.*, around day of the year 307±5 days). Schmidt stability reflected these dynamics and reached very high numbers in summer (>2475 J m^{-2}) which prevents any substantial warming in deep waters (*i.e.*, >30 m depth) during the summer season. By comparison, Schmidt stability was far lower during winter (Fig. 7) reflecting the typical situation in dimictic lakes that the stability of the winter inversed stratification was not as high (35 J m^{-2}) as during summer stratification. According to the simulation results, winter inverse stratification in Lake Sevan is initiated approximately at day of the year 10±6 days and ceases at day of the year 90±12 days. However, this stratification is often ephemeral and can only persist if cold temperature prevails over longer periods while any warming event is rather quickly destroying inverse stratification leading to intermittent mixing. The average duration of uninterrupted inverse stratification is about 3 weeks, starting from day of the year 28±16 until day of the year 50±21. The model output showed the formation of ice cover in two years; 2008 with a maximum thickness of 16.3 cm for a duration of 46 days between day of the year 24 until 70, and in 2017 with a maximum thickness of 11.5 cm for a duration of 42 days between day of the year 42 until 84.

Although the simulated water temperatures using EWEMBI resembled the temperatures in the averaged measured meteorology simulation, the simulated duration of summer stratification in the EWEMBI-driven simulation was about 10% longer, which could be attributed to the underestimation of wind speed (Tab. 2). The general pattern in stratification phenology was, nevertheless, nearly the same (Fig. 7). When comparing EWEMBI-based simulation outputs with those obtained from local meteorology it appeared that EWEMBI works quite well during the warmer season but has some problems during the cold season, which is also reflected by the slight shifts in stratification onset/offset in Fig. 7.

Climate sensitivity scenarios

The gradual increase of air temperature by 1 to 5 K translated into an increase in the summer surface water temperature (Figs. 8 and 9) in a linear manner. Per 1 K warmer air temperature the surface water temperature warmed by approximately 0.8 K (Fig. 9). While warming in the epilimnion was closely connected to air temperature, the reaction of the hypolimnetic temperatures was weaker (Fig. 8). Following the changes in surface water temperature, the onset of stratification was advanced under warming and the stratification end was delayed resulting in markedly extended stratification durations. For example, the stratification started 21 days earlier and ended 8 days later in the +5K scenario compared to the current climate, resulting in 29 days, *i.e.*, almost one month, of extended stratification duration. This corresponds to an almost 15% increase (Fig. 9). This result indicated that the stratification onset reacted more sensitively to warming than the end of the stratification, *i.e.,* effects from global warming were stronger in spring than in late autumn. Moreover, not only the stratification duration increased (compared to an average of 188 days under current climate settings), but also the stratification became stronger as indicated by increasing Schmidt stability during the summer season from 1900 J m^{-2} (average from June to August) under the current climate to 3000 J m^{-2} for the +5K scenario. The mixing layer depth, however, appeared to be rather stable over all warming scenarios and remained between 7 and 8 m (Fig. 9).

The stratification also reacted sensitively to changing wind speed. Higher wind speeds increase surface mixing and intensify non-radiative heat fluxes, leading to decreased surface water temperatures and deeper mixing depth during summer stratification (Figs. 8 and 9). This cooling effect of wind was mostly driven by intensifying latent heat loss due to evaporation with increasing wind while sensible heat fluxes can be positive (during hot days) or negative (during cold nights). Nevertheless, latent heat fluxes are almost always higher in absolute value as sensible heat fluxes as reflected by calculated Bowen ratios (*i.e.*, ratio of sensible over latent heat flux) remaining between -1 and +1. So, even in winter times the evaporative cooling effect is larger than the heat loss by sensible heat and intensifying wind is intensifying this heat loss. The impacts of these scenarios on stratification could be noticed by decreasing stratification length by 37 days when the wind factors increased from 0.8 to 1.2, corresponding to a 21% decrease. While stratification onset was delayed by 20 days, the stratification end was shifted 17 days earlier. Schmidt stability demonstrated comparatively small changes despite the decrease of surface temperature because of deepening of the mixing layer by about 5 m when wind factor increases from 0.8 to 1.2. We conclude that Lake Sevan reacts quite sensitively to relatively moderate changes in wind speed of ±20%.

DISCUSSION

In this study, the 1D hydrodynamic model GLM was applied to study Lake Sevan's thermal dynamics. Based on a simulation over one decade (from 2008-2017) in which measurements of water temperature at distinct depths were available, we were able to systemically assess the performance of the model. The results showed that our model reproduced all stratification and mixing patterns with high accuracy. With an overall average RMSE of 1.56°C and average bias of 0.05°C these measures of fit

were in a range that was also obtained in comparable studies (Fenocchi *et al.*, 2017; Weber *et al.,* 2017; Bruce *et al.,* 2018). This provides the first model-based analysis of hydrodynamics and stratification in this large mountain lake and highly relevant freshwater resource.

Nonetheless, the results of the simulations are associated with uncertainties induced by multiple sources. The meteorological input data have to be mentioned here in the first line as the meteorological conditions around the lake are heterogeneous and the landscape morphology is complex. The large surface area of the lake makes it unlikely that meteorological conditions are really uniform over the entire lake, we rather have to expect that local weather phenomena (*e.g.*, sea-land-breeze) and orographic effects to play a significant role (compare Gevorgyan, 2018). The application of one spatially uniform meteorological input data set, as usual for 1D lake models, is therefore a major simplification and should lead to some compromises in model accuracy. The same argument holds true for the spatial heterogeneities within this large water body as illustrated in Fig. 5, *i.e.*, the differences between water temperatures measured at the same depth and date in the two sub-basins

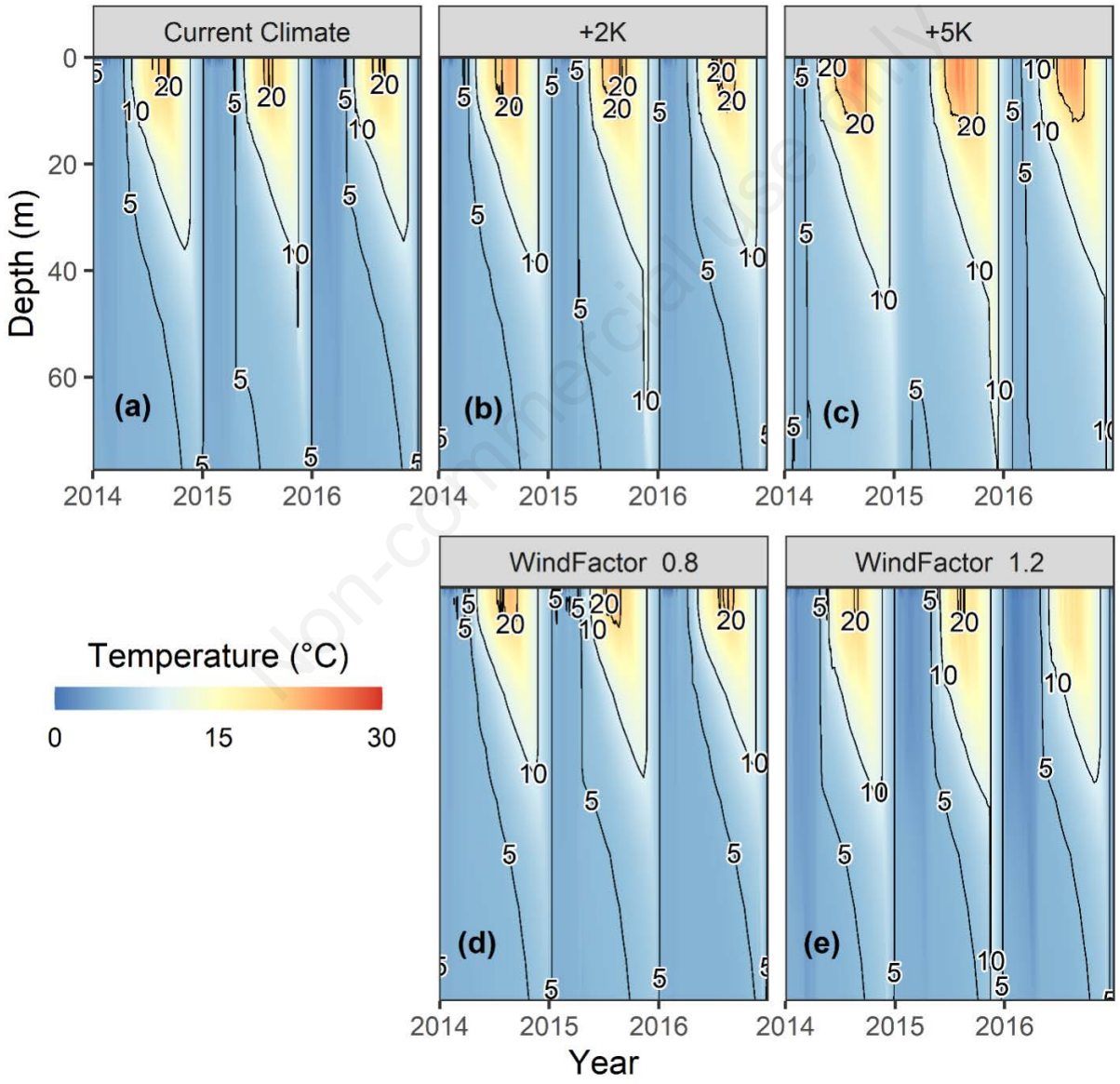

Fig. 8. Results of simulations analysing the sensitivity of Lake Sevan water temperatures against warming and changing wind speed. The plot only shows the years 2015-2016 and the 20, 10 and 5°C isotherm lines. The respective scenarios are shown above the plot: a) reference simulation; b,c) warming scenarios; d,e) wind scenarios.

Small and Big Sevan. Another factor influencing the thermal dynamics and the biological process may be water transparency (Rinke *et al*., 2010; Shatwell *et al*., 2016), which was assigned to a constant value during the simulation period. This value, however, is changing over time and is different between the two sub-basins (Gevorgyan *et al*., 2020) implying another source of uncertainty. Taken together, we expected some level of residual variability between model and observation and having this in mind the achieved RMSE and very low bias indicate that GLM performs reasonably well for Lake Sevan. This not only confirms the transferability of the model but also supports the usage of GLM as a modelling tool in climate change studies or lake management applications.

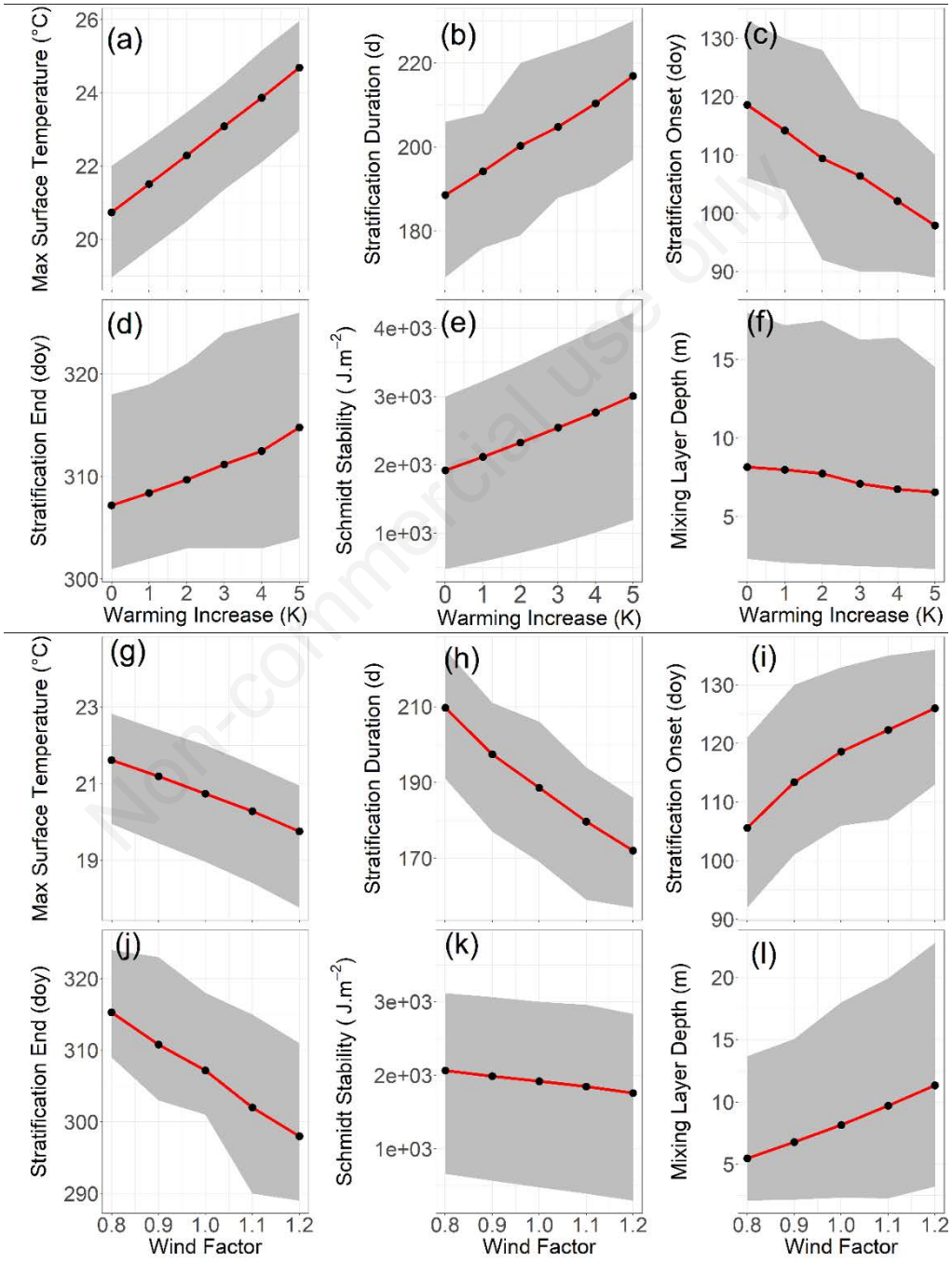

Fig. 9. The average and range of stratification indices for Lake Sevan under warming and wind scenarios. The red line represents the mean of the 10 years while the shaded grey area displays the inter-annual variability as range. a-f) Warming scenarios. g-l) Wind

It is possible to overcome the limitations mentioned above by using a lake model with a higher spatial resolution, *i.e.,* a 3D lake model that can account for the complex morphometry of Lake Sevan and the complex wind field. Applications of 3D models in large lakes and reservoirs clearly documented their abilities to capture spatial heterogeneities as well as the complex hydrodynamic patterns and processes that arise from 3D effects (Baracchini *et al*., 2020; Bocaniov *et al*., 2020, 2014). A better understanding of the two basins' exchange mechanisms, for example, would be an important aspect of such a 3D model application because most inflows and the major pollution sources enter the sub-basin of Big Sevan while the outlet is leaving the lake at the northern end of Small Sevan. A 3D model would then be useful to study the transport and distribution of pollutants within the lake. If coupled with an ecological lake model, such a 3D lake model could even provide predictions for the fate of nutrients, biogeochemical processing with major elemental cycles or the occurrence of eutrophication effects.

Our study also enabled a detailed analysis of the sensitivity of Lake Sevan's stratification phenology against climatic conditions. We applied the calibrated model in order to analyse the response of thermal dynamics to climate warming and changing wind conditions. Although climate change will ultimately affect all meteorological variables, air temperature and wind speed were shown to be of primary influence for lake physics (Dong *et al*., 2020; Woolway *et al*., 2019; Woolway and Merchant, 2019). It is therefore reasonable to focus an initial assessment of climate impact on lakes on these variables. Moreover, the fact that the physical structure of Lake Sevan reacted with distinct changes in response to changing wind and air temperature conditions, *e.g.,* with respect to stratification onset and end or mixing depth, supported our approach. The changes in stratification phenology predicted for warming scenarios are in line with other studies that show that stratification onset advances faster than stratification end is delayed (Magee and Wu, 2017; Woolway and Merchant, 2018). Moreover, the water temperature trend of 80% of the warming trend in air temperature agrees to other modelling studies in temperate lakes (Shatwell *et al*., 2019).

Finally, our study enabled a multi-decadal simulation of Lake Sevan (from 1979-2016) by using a freely available global meteorological data product (EWEMBI, see Lange, 2019). These gridded data require spatial interpolation before application but do not need to be bias-corrected because they amalgamate reanalysis with observational data. A comparison of the EWEMBI-data with local observations in the period 2008-2016 demonstrated that both were in good agreement with each other (Tab. 2), in particular with respect to the major thermal energy-delivering variables air temperature and solar radiation. Poorer agreement was achieved for such variables as cloud cover, precipitation and wind speed that are more strongly influenced by local features (*e.g.*, orography, land-water-interactions, etc.) although their bias was still low and therefore, we believe they are still well suited for being input into lake models. The simulation of these almost four decades provided important information on the natural variability in climatic conditions and the corresponding physical structure of the lake. Such data are required for a sound assessment of climate impacts because any change in climatic conditions has to be interpreted against the background of climate variability at a given site. Moreover, this multi-decadal simulation showed that Lake Sevan is warming more slowly than many temperate lakes. For referencing, O'Reilly *et al*., (2015) estimated median warming values for temperate lakes of 0.48°C decade^{-1} for ice-covered and for warm-winter 0.25°C decade^{-1}. For detailed analysis of the meteorological trends and seasonality in the region see (Gevorgyan, 2014).

Climate change impacts on Lake Sevan and its ecosystem

Our results provided evidence that under future climate conditions Lake Sevan will experience prolonged stratification periods and more stable stratification. With the progression of climate warming, winter inverse stratification will become weaker, until it disappears in the +4 and +5K scenarios. This means Lake Sevan will shift from a dimictic to a monomicitic mixing type. The impacts from changing thermal conditions will affect the ecosystem dynamics and water quality of this outstanding mountain freshwater ecosystem, as well. In the forefront, we expect increasing risks of oxygen depletion in the hypolimnion, as documented by other studies (Schwefel *et al*., 2016). The sediment-water contact zone currently experiences hypoxia at the end of the stratification period (unpublished measurements in Oct 2018), but the hypolimnion as a whole is still well oxygenated. A loss of deep water oxygen would have severe consequences for Lake Sevan: i) loss of current hypolimnetic benthic and planktonic communities with negative effects on biodiversity, ii) reduced phosphorus retention by sediments and higher phosphorus release at the sediment-water-interface (Hupfer and Lewandowski, 2008), and iii) lower mineralization capacity of organic matter and accumulation of reduced substances in the sediments (Steinsberger *et al*., 2021).

Negative effects of climate change are in many ways similar to the effects from eutrophication, as stated in a seminal paper from Moss *et al*., (2011), *e.g.* dominance of cyanobacteria, declining biodiversity, rising nutrient levels, and productivity as well as hypolimnetic anoxia. It is therefore hazardous when warming and eutrophication act in parallel on a given lake ecosystem. Unfortu-

nately, Lake Sevan already shows clear signs of eutrophication (Gevorgyan *et al*., 2020). This calls for immediate intervention by the management boards and a long-term strategy is required to restrict nutrient input to the lake to remain within acceptable limits in order to maintain the services provided by the lake (*i.e.*, water supply, tourism, fishing and growing livestock, biodiversity, nutrient retention, *etc*.).

Further research based on the established Lake Sevan model

The achieved state of lake modelling in Lake Sevan provides new options for sustaining and understanding Lake Sevan, which is currently seen as an ecosystem at risk. Though this list is not exhaustive, we basically want to emphasize three lines of future research: i) including water quality and biogeochemical processing into the model, ii) providing more advanced climate projections including uncertainties and different carbon emission pathways, and iii) linking the lake model to a hydrological catchment model.

The recent water quality deteriorations (Gevorgyan *et al*., 2020) in Lake Sevan call for management interventions and nutrient control. Such management strategies require a scientific basis and quantitative information about management targets. Such information cannot be provided by a physical lake model but require an ecological lake model. The applied model in this study, GLM, can be coupled to an ecological lake model (AED – Aquatic Ecosystem Dynamics) and simulate phytoplankton dynamics, nutrient cycling and oxygen dynamics (*e.g.*, see Snortheim *et al*., 2017). Such a model system could then, for example, provide estimates for critical nutrient loading thresholds that prevent algal blooms or hypolimnetic anoxia and by that would automatically bridge to lake management strategies and ecosystem services. A major benefit of such an approach would be that the response of the water quality variables *(e.g.*, oxygen, nutrients, and algae groups) to global warming trends can be fully integrated into the setting (Snortheim *et al*., 2017).

Although our study already provided concrete insights into the reaction of Lake Sevan to climate warming, the applied approach was simple. Future work should account for uncertainties and be based on projections from Global Circulation Models (GCMs) and Regional Climate Models (RCMs). This is the case because they can account for seasonality, geographical effects and include specific assumptions on carbon emission pathways. Employing multiple GCMs will enable ensemble simulations and, by that, provide model-based uncertainty estimates, while the simulation of different climate scenarios (Representative Concentration Pathways: RCP 2.6, 4.5, and 8.5, see IPCC, 2014) can account for uncertainties in future climate change mitigation policies. Such ensemble data sets for different climate scenarios are available at the global scale, *e.g.*, by repositories provided by ISIMIP (Warszawski *et al*., 2014) or regionally like CORDEX (Gutowski Jr. *et al*., 2016) . The multi-decadal simulations in our study driven by the gridded EWEMBI data, which is a product that merges reanalysis and meteorological forcing, could be of use for such an approach, *e.g.*, for benchmarking and, if needed, bias correction.

Lake Sevan is located in an arid climate resulting in high evaporative losses from the water surface. In addition, Lake Sevan has a catchment area of 4712 km^2, and the ratio of catchment area to lake surface area computes to approximately 3.7. This is a rather small value compared to many other lakes of this size, illustrating that the water delivery into the lake is small. These facts are also mirrored by the very long residence time as outlined in the study site description above. Induced by climate warming, increasing evaporative losses from both the lake's surface and the catchment area, will most likely prolong residence times in Lake Sevan even more within this century. We recommend detailed projections for discharge development and catchment hydrology and hence recommend establishing a hydrological model for the Lake Sevan catchment and use the outputs from this model as hydrological inputs into the lake model. This knowledge is important for lake management, not only because it informs future water availability but also because new risks may arise from these developments. These risks include, for example, salinization, increasing susceptibility against pollution, and longer response times to water quality improvements in the inflows resulting from lower flushing. Reduction of water withdrawals from the lake will be a primary consequence, which will affect hydropower gains and water availability in the fertile lands downstream.

Last but not least, we want to stress the importance of lake monitoring of this sensitive large mountain lake. Reliable lake management plans require knowledge and this can only be extracted if the appropriate data have been collected. The monitoring data were also a decisive aspect of this modeling study and will become even more important if GLM is expanded in order to include also water quality and ecosystem dynamics. Moreover, a long-term monitoring perspective is also important for lake managers to assess the effects of certain measures taken in the lake or its catchment. Finally, the monitoring would facilitate establishing a real-time modeling system including a lake model and real-time weather monitoring/forecast that would provide managers and decision makers with important operational information. We therefore conclude our article with a devoted plea to maintain and expand the current monitoring activities on Lake Sevan and to provide a long-term management strategy that keeps this unique ecosystem in good health.

ACKNOWLEDGEMENTS

We thank Olaf Büttner and Philipp Keller for their help with preprocessing the geodata. And Robert Ladwig for his advices on model calibration. We thank Bertram Boehrer and Bardukh Gabrielyan for helpful discussions. The Hydrometeorology and Monitoring Center state non-commercial organization of the Ministry of Environment of the Republic of Armenia (HMC) (Yerevan, Armenia) provided the hydrological and meteorological data. We thank the German Federal Ministry of Education and Research for financial support provided within the project SevaMod (grant number 01DK17022) and GlobWQ (grant number 02WGR1527A). The Open Access publication of this article was financially supported by the German Federal Ministry of Education and Research (grant number 16PGF0353). Chenxi Mi is also supported by the National Natural Science Foundation of China (42107060). We thank three anonymous reviewers for the time and effort they have dedicated to providing valuable and critical feedback on the manuscript. We thank the HMC for their permission to make the data and the model setup openly available at https://pangaea.de/?t=Lakes+%26+Rivers under the same name of the manuscript. EWEMBI data can be retrieved from https://esg.pik-potsdam.de/search/isimip/?project= ISIMIP2b&dataset_type=Climate+atmosphere+observed.

REFERENCES

Andréassian V, Gevorgyan A, Azizyan L, Misakyan A, Khalatyan Y, Melkonyan H, Misakyan E, Piliposyan N, Azizyan H. Climate elasticity of Lake Sevan inflow. J. Limnol. (in press).

Baracchini T, Wüest A, Bouffard D, 2020. Meteolakes: An operational online three-dimensional forecasting platform for lake hydrodynamics. Water Res. 172:115529.

Berger SA, Diehl S, Stibor H, Sebastian P, Scherz A, 2014. Separating effects of climatic drivers and biotic feedbacks on seasonal plankton dynamics: no sign of trophic mismatch. Freshwater Biol. 59:2204–2220.

Bocaniov SA, Lamb KG, Liu W, Rao YR, Smith REH, 2020. High Sensitivity of lake hypoxia to air temperatures, winds, and nutrient loading: Insights from a 3-D lake model. Water Resour. Res. 56:e2019WR027040.

Bocaniov SA, Ullmann C, Rinke K, Lamb KG, Boehrer B, 2014. Internal waves and mixing in a stratified reservoir: Insights from three-dimensional modeling. Limnologica 49:52-67.

Boehrer B, Schultze M, 2008. Stratification of lakes. Rev. Geophys. 46:RG2005.

Bruce LC, Frassl MA, Arhonditsis GB, Gal G, Hamilton DP, Hanson PC, Hetherington AL, Melack JM, Read JS, Rinke K, Rigosi A, Trolle D, Winslow L, Adrian R, Ayala AI, Bocaniov SA, Boehrer B, Boon C, Brookes JD, Bueche T, Busch BD, Copetti D, Cortés A, de Eyto E, Elliott JA, Gallina N, Gilboa Y, Guyennon N, Huang L, Kerimoglu O, Lenters JD, MacIntyre S, Makler-Pick V, McBride CG, Moreira S, Özkundakci D, Pilotti M, Rueda FJ, Rusak JA, Samal NR, Schmid M, Shatwell T, Snorthheim C, Soulignac F, Valerio G, van der Linden L, Vetter M, Vinçon-Leit, B, Wang J, Weber M, Wickramaratne C, Woolway RI, Yao H, Hipsey MR, 2018. A multi-lake comparative analysis of the General Lake Model (GLM): Stress-testing across a global observatory network. Environ. Model. Softw. 102:274–291.

Bueche T, Hamilton DP, Vetter M, 2017. Using the General Lake Model (GLM) to simulate water temperatures and ice cover of a medium-sized lake: a case study of Lake Ammersee, Germany. Environ. Earth Sci. 76:461.

Dong F, Mi C, Hupfer M, Lindenschmidt K-E, Peng W, Liu X, Rinke K, 2020. Assessing vertical diffusion in a stratified lake using a three-dimensional hydrodynamic model. Hydrol. Process. 34:1131–1143.

Fang X, Stefan HG, 2009. Simulations of climate effects on water temperature, dissolved oxygen, and ice and snow covers in lakes of the contiguous U.S. under past and future climate scenarios. Limnol. Oceanogr. 54:2359–2370.

Farrell KJ, Ward NK, Krinos AI, Hanson PC, Daneshmand V, Figueiredo RJ, Carey CC, 2020. Ecosystem-scale nutrient cycling responses to increasing air temperatures vary with lake trophic state. Ecol. Model. 430:109134.

Fenocchi A, Rogora M, Sibilla S, Ciampittiello M, Dresti C, 2018. Forecasting the evolution in the mixing regime of a deep subalpine lake under climate change scenarios through numerical modelling (Lake Maggiore, Northern Italy/Southern Switzerland). Clim. Dyn. 51:3521–3536.

Gabrielyan B, Khosrovyan A, Schultze M (2022). A review of anthropogenic stressors on Lake Sevan. J. Limnol. 81:2061.

Gevorgyan A, 2014. Surface and tropospheric temperature trends in Armenia. Int. J. Climatol. 34:3559–3573.

Gevorgyan A, 2018. Convection-permitting simulation of a heavy rainfall event in Armenia using the WRF model. J. Geophys. Res. Atmospheres 123:11008-11029.

Gevorgyan A, Melkonyan H, 2015. Regional impact of the Armenian highland as an elevated heat source: ERA-Interim reanalysis and observations. Clim. Dyn. 44:1541–1565.

Gevorgyan A, Melkonyan H, Aleksanyan T, Iritsyan A, Khalatyan Y, 2016. An assessment of observed and projected temperature changes in Armenia. Arab. J. Geosci. 9:27.

Gevorgyan G, Rinke K, Schultze M, Mamyan A, Kuzmin A, Belykh O, Sorokovikova E, Hayrapetyan A, Hovsepyan A, Khachikyan T, Aghayan S, Fedorova G, Krasnopeev A, Potapov S, Tikhonova I, 2020. First report about toxic cyanobacterial bloom occurrence in Lake Sevan, Armenia. Int. Rev. Hydrobiol. 105:131–142.

Gutowski Jr WJ, Giorgi F, Timbal B, Frigon A, Jacob D, Kang H-S, Raghavan K, Lee B, Lennard C, Nikulin G, O'Rourke E, Rixen M, Solman S, Stephenson T, Tangang F, 2016. WCRP COordinated Regional Downscaling EXperiment (CORDEX): a diagnostic MIP for CMIP6. Geosci. Model Dev. 9:4087–4095.

Hansen N, 2016. The CMA Evolution Strategy: A Tutorial. ArXiv160400772 Cs Stat.

Hayes NM, Haig HA, Simpson GL, Leavitt PR, 2020. Effects of lake warming on the seasonal risk of toxic cyanobacteria exposure. Limnol. Oceanogr. Lett. 5:393–402.

Hipsey MR, Bruce LC, Boon C, Busch B, Carey CC, Hamilton DP, Hanson PC, Read JS, de Sousa E, Weber M, Winslow LA, 2019. A General Lake Model (GLM 3.0) for linking with high-frequency sensor data from the Global Lake Ecological Observatory Network (GLEON). Geosci. Model Dev. 12:473–523.

Ho JC, Michalak AM, Pahlevan N, 2019. Widespread global increase in intense lake phytoplankton blooms since the 1980s. Nature 574:667–670.

Hovanesian R, Bronozian H, 1994. Restoration and management of Lake Sevan in Armenia: Problems and prospects. Lake Reserv. Manag. 9:178–182.

Hovhanissian R, Gabrielyan B, 2000. Ecological problems associated with the biological resource use of Lake Sevan, Armenia. Ecol. Eng. 16:175–180.

Hupfer M, Lewandowski J, 2008. Oxygen controls the phosphorus release from lake sediments – a long-lasting paradigm in limnology. Int. Rev. Hydrobiol. 93:415–432.

Idso SB, 1973. On the concept of lake stability. Limnol. Oceanogr. 18:681–683.

IPCC, 2014. Climate Change 2014: Synthesis Report. Contribution of Working Groups I, II and III to the Fifth Assessment Report of the Intergovernmental Panel on Climate Change. IPCC, Geneva. 151 pp.

Iturbide M, Bedia J, Herrera S, Baño-Medina J, Fernández J, Frías MD, Manzanas R, San-Martín D, Cimadevilla E, Cofiño AS, Gutiérrez JM, 2019. The R-based climate4R open framework for reproducible climate data access and post-processing. Environ. Model. Softw. 111:42–54.

Kasten F, Czeplak G, 1980. Solar and terrestrial radiation dependent on the amount and type of cloud. Sol. Energy 24:177–189.

Kerimoglu O, Rinke K, 2013. Stratification dynamics in a shallow reservoir under different hydro-meteorological scenarios and operational strategies. Water Resour. Res. 49:7518–7527.

Kirillin G, 2010. Modeling the impact of global warming on water temperature and seasonal mixing regimes in small temperate lakes. Boreal Env. Res. 15:279–293.

Ladwig R, Furusato E, Kirillin G, Hinkelmann R, Hupfer M, 2018. Climate change demands adaptive management of urban lakes: Model-based assessment of management scenarios for Lake Tegel (Berlin, Germany). Water 10:186.

Ladwig R, Hanson PC, Dugan HA, Carey CC, Zhang Y, Shu L, Duffy CJ, Cobourn KM, 2021. Lake thermal structure drives interannual variability in summer anoxia dynamics in a eutrophic lake over 37 years. Hydrol. Earth Syst. Sci. 25:1009–1032.

Lange S, 2019. EartH2Observe, WFDEI and ERA-Interim data Merged and Bias-corrected for ISIMIP (EWEMBI). GFZ Data Services.

Magee MR, Wu CH, 2017. Response of water temperatures and stratification to changing climate in three lakes with different morphometry. Hydrol. Earth Syst. Sci. 21:6253–6274.

Mesman JP, Ayala,AI, Adrian R, De Eyto E, Frassl MA, Goyette S, Kasparian J, Perroud M, Stelzer JAA, Pierson DC, Ibelings BW, 2020. Performance of one-dimensional hydrodynamic lake models during short-term extreme weather events. Environ. Model. Softw. 133:104852.

Mi C, Frassl MA, Boehrer B, Rinke K, 2018. Episodic wind events induce persistent shifts in the thermal stratification of a reservoir (Rappbode Reservoir, Germany). Int. Rev. Hydrobiol. 103:71–82.

Mi C, Shatwell T, Ma J, Xu Y, Su F, Rinke K, 2020. Ensemble warming projections in Germany's largest drinking water reservoir and potential adaptation strategies. Sci. Total Environ. 748:141366.

Michalsky JJ, 1988. The Astronomical Almanac's algorithm for approximate solar position (1950–2050). Sol. Energy 40:227–235.

Moore TN, Mesman JP, Ladwig R, Feldbauer J, Olsson F, Pilla RM, Shatwell T, Venkiteswaran JJ, Delany AD, Dugan H, Rose KC, Read JS, 2021. LakeEnsemblR: An R package that facilitates ensemble modelling of lakes. Environ. Model. Softw. 143:05101.

Moss B, Kosten S, Meerhoff M, Battarbee RW, Jeppesen E, Mazzeo N, Havens K, Lacero, G, Liu, Z, Meester LD, Paerl H, Scheffer M, 2011. Allied attack: climate change and eutrophication. Inland Waters 1:101–105.

North RP, North RL, Livingstone DM, Köster O, Kipfer R, 2014. Long-term changes in hypoxia and soluble reactive phosphorus in the hypolimnion of a large temperate lake: consequences of a climate regime shift. Glob. Change Biol. 20:811-823.

O'Reilly CM, Sharma S, Gray DK, Hampton SE, Read JS, Rowley RJ, Schneider P, Lenters,JD, McIntyre PB, Kraemer BM, Weyhenmeyer GA, Straile D, Dong B, Adrian R, Allan MG, Anneville O, Arvola L, Austin J, Bailey JL, Baron JS, Brooke, JD, de Eyto E, Dokulil MT, Hamilton DP, Havens K, Hetherington AL, Higgins SN, Hook S, Izmest'eva LR, Joehnk KD, Kangur K, Kasprzak P, Kumagai M, Kuusisto E, Leshkevich G, Livingstone DM, MacIntyre S, May L, Melack JM, Mueller-Navarra DC, Naumenko M, Noges P, Noges T, North, RP, Plisnier P-D, Rigosi A, Rimmer A, Rogora M, Rudstam LG, Rusak JA, Salmaso N, Samal NR, Schindler DE, Schladow SG, Schmid M, Schmidt SR, Silow E, Soylu ME, Teubner K, Verburg P, Voutilainen A, Watkinson A, Williamson CE, Zhang G, 2015. Rapid and highly variable warming of lake surface waters around the globe. Geophys. Res. Lett. 42:10773-10781.

Paerl HW, Huisman J, 2008. Blooms like it hot. Science 320: 57–58.

Poddubny SA, 2010. [Hydrophysical characterization of the water column], p. 41–47. In: D.S. Pavlov, A.V. Krylov, B.K. Gabirleyan and S.A. Poddubny (eds.), [Ecology of Lake Sevan during the period of water level rise. The results of Russian-Armenian biological expedition for hydroecological survey of Lake Sevan (Armenia) (2005–2009)].[Book in Russian]. Nauka DNC, Makhachkala.

Poole HH, Atkins WRG, 1929. Photo-electric measurements of submarine illumination throughout the year. J. Mar. Biol. Assoc. UK 16:297–324.

R Core Team, 2021. R: A Language and Environment for Statistical Computing. R Foundation for Statistical Computing, Vienna.

Rinke K, Yeates P, Rothhaupt K-O, 2010. A simulation study of the feedback of phytoplankton on thermal structure via light extinction. Freshwater Biol. 55:1674–1693.

RStudio Team, 2021. RStudio: Integrated Development Environment for R. RStudio, PBC, Boston.

Schmidt W, 1928. [Über Die Temperatur- Und Stabilitätsverhältnisse von Seen].[Article in German]. Geogr. Ann. 10:145–177.

Schwefel R, Gaudard A, Wüest A, Bouffard D, 2016. Effects of climate change on deepwater oxygen and winter mixing in a deep lake (Lake Geneva): Comparing observational findings and modeling. Water Resour. Res. 52:8811–8826.

Sen PK, 1968. Estimates of the regression coefficient based on Kendall's Tau. J. Am. Stat. Assoc. 63:1379–1389.

Shatwell T, Adrian R, Kirillin G, 2016. Planktonic events may cause polymictic-dimictic regime shifts in temperate lakes. Sci. Rep. 6:24361.

Shatwell T, Thiery W, Kirillin G, 2019. Future projections of temperature and mixing regime of European temperate lakes. Hydrol. Earth Syst. Sci. 23:1533–1551.

Snortheim CA, Hanson PC, McMahon KD, Read JS, Carey CC, Dugan HA, 2017. Meteorological drivers of hypolimnetic anoxia in a eutrophic, north temperate lake. Ecol. Model. 343:39–53.

Steinsberger T, Wüest A, Müller B, 2021. Net ecosystem production of lakes estimated from hypolimnetic organic carbon sinks. Water Resour. Res. 57:e2020WR029473.

Swinbank WC, 1963. Long-wave radiation from clear skies. Q. J. R. Meteorol. Soc. 89:339–348.

Vardanyan L, Azizyan L, Yeroyan Y, Danielyan A, 2014. The change of water resources in Lake Sevan in the context of climate change renewed scenarios, p. 123–128. In: Proceedings AASSA Regional Workshop/ Compilation by M. Nalbandyan and Armine Avetisyan; Institute of Geological Sciences of the National Academy of Sciences of the Republic of Armenia, Yerevan.

Vermishev M, Papyan S, Gabrielyan A, Harutyunyan D, Vahradyan T, 2015. Armenia's Third National Communication on Climate Change. Republic of Armenia, Ministry of Nature Protection. Lusabats Publishing House, Yerevan.

Warszawski L, Frieler K, Huber V, Piontek F, Serdeczny O, Schewe J, 2014. The Inter-Sectoral Impact Model Intercomparison Project (ISI–MIP): Project framework. Proc. Natl. Acad. Sci. 111:3228–3232.

Weber M, Boehrer B, Rinke K, 2019. Minimizing environmental impact whilst securing drinking water quantity and quality demands from a reservoir. River Res. Appl. 35:365–374.

Wilson HL, Ayala AI, Jones ID, Rolston A, Pierson D, de Eyto E, Grossart H-P, Perga M-E, Woolway RI, Jennings E, 2020. Variability in epilimnion depth estimations in lakes. Hydrol Earth Syst Sci 24:5559–5577.

Winslow L, Read J, Woolway R, Bentrup J, Leach T, Zwart J. 2014. rLakeAnalyzer: Package for the analysis of lake physics. R package, Version 1.4.

Woolway RI, Jennings E, Shatwell T, Golub M, Pierson DC, Maberly SC, 2021. Lake heatwaves under climate change. Nature 589:402–407.

Woolway RI, Merchant CJ, 2018. Intralake Heterogeneity of thermal responses to climate change: A Study of large northern hemisphere lakes. J. Geophys. Res. Atmos. 123:3087–3098.

Woolway RI, Merchant CJ, 2019. Worldwide alteration of lake mixing regimes in response to climate change. Nat. Geosci. 12:271–276.

Woolway RI, Merchant CJ, Hoek JVD, Azorin-Molina C, Nõges P, Laas A, Mackay EB, Jones ID, 2019. Northern hemisphere atmospheric stilling accelerates lake thermal responses to a warming world. Geophys. Res. Lett. 46:11983–11992.

Yu W, Cestti RE, Lee JY, 2014. Toward integrated water resources management in Armenia. The World Bank.